

# Fabrication of periodically poled lithium tantalate for UV generation with diode lasers

J.-P. Meyn<sup>1,\*</sup>, C. Laue<sup>1,\*\*</sup>, R. Knappe, R. Wallenstein<sup>1</sup>, M.M. Fejer<sup>2</sup>

<sup>1</sup>Fachbereich Physik, Universität Kaiserslautern, Erwin-Schrödinger-Strasse 46, 67663 Kaiserslautern, Germany  
(Fax: +49-631/205-3906, E-mail: meyn@physik.uni-kl.de)

<sup>2</sup>Stanford University, E.L. Ginzton Laboratory, Stanford, CA 94305-4085, USA

Received: 11 June 2001/Published online: 18 July 2001 – © Springer-Verlag 2001

**Abstract.** Fabrication of periodically poled lithium tantalate (PPLT) with periods as short as 1.3  $\mu\text{m}$  for second harmonic generation (SHG) in the UV range and for optical parametric oscillators pumped at 532 nm is reported. Both the maximum crystal size of up to 40 mm and the minimum poling period of 1.3  $\mu\text{m}$  are improvements on earlier results, achieved by optimizing the poling conditions and by using a novel electrode design consisting of electrode structures on both surfaces of the crystal. Single-pass SHG of a master oscillator power amplifier (MOPA) diode laser with an output power of 1.36 mW at 336 nm using a 16-mm-long PPLT crystal with a 1.5  $\mu\text{m}$  poling period is reported.

**PACS:** 42.65.Jx; 42.70.Mp; 77.84.Dy

The development of quasi-phase-matched (QPM) materials has led to significant progress in the field of nonlinear optics due to the versatility of this concept [1, 2]. Several materials have been investigated and compared in recent years, and a huge number of publications in many fields of nonlinear optics have appeared. Nonlinear optical frequency conversion in the UV is primarily realized in birefringent materials such as barium beta borate,  $\text{BaB}_2\text{O}_4$  (BBO), Lithium triborate,  $\text{LiB}_3\text{O}_5$  (LBO) and new borates. For QPM crystals, the main problem is the fabrication of a periodic structure with a period typically less than 2  $\mu\text{m}$  in a bulk crystal of sufficient thickness, at least 200  $\mu\text{m}$ . Another issue is the limited UV transparency range of many ferroelectrics. Nevertheless recent progress in material fabrication has made QPM materials very attractive for certain applications in the UV range.

Periodically poled lithium niobate (PPLN) [3, 4] is commonly used due to its highly effective nonlinear coefficient,  $d_{\text{eff}} = 17 \text{ pm/V}$ , the available crystal length of up to 90 mm, and its excellent mechanical stability. The fabrication of QPM periods smaller than 2  $\mu\text{m}$  as is necessary for second harmonic generation (SHG) in the UV range remains challenging; however, significant progress has been demonstrated with 4  $\mu\text{m}$  pitch gratings for SHG in the visible spectral range [5].

Periodically poled potassiumtitanyl phosphate,  $\text{KTiOPO}_4$ , (PPKTP) is interesting because it exhibits no photorefractive effects and therefore can be used at room temperature. PPKTP has been used for SHG in the near UV [6]; however, its transparency range ends at 350 nm [7], and the limited reproducibility of the ferroelectric properties associated with the crystal growth technique from a flux is a severe problem for fabricating short pitch QPM gratings in PPKTP.

Periodically poled lithium tantalate (PPLT) is attractive for efficient SHG into the UV spectral range because it has the largest transparency range, down to 280 nm among the known ferroelectrics. Moreover, the fabrication of very short pitch QPM gratings is possible, which is necessary to compensate for the large dispersion in the UV. Single-pass SHG in PPLT with periods down to 1.7  $\mu\text{m}$  [8], wavelengths down to 325 nm [9], and output power up to 56 mW at 38% conversion efficiency [10] have been demonstrated.

We present a detailed report on the fabrication and characterisation of PPLT with short QPM periods, below 2  $\mu\text{m}$ .

## 1 Ferroelectric properties

The ferroelectric properties of lithium tantalate with congruently melting composition are similar to those of lithium niobate, which have been studied in great detail [11]. The coercive field is 21 kV/mm. The domain wall shape and the nucleation density for domains is different in lithium tantalate [12], necessitating a different fabrication procedure.

The domains poled in homogeneous lithium tantalate have triangular shape, as opposed to the hexagonal shape of domains in lithium niobate. On the one hand, this is a disadvantage, because it is difficult to obtain straight domain walls, in particular in the regions away from the surface electrodes. On the other hand, the reduction of wall energy when domains are touching each other is less pronounced, and thus the domains have much less tendency to merge. The orientation of the crystal relative to the domain grating has a significant influence on the domain wall quality, as shown in Fig. 1. The domains have been revealed by etching in hydrofluoric acid (HF, 48%) for 30 min at room temperature. In all cases, the domains are straight and periodic on the  $c+$  face, but split

\*Corresponding author.

\*\*Present address: IBM Speichersysteme GmbH, 55131 Mainz, Germany

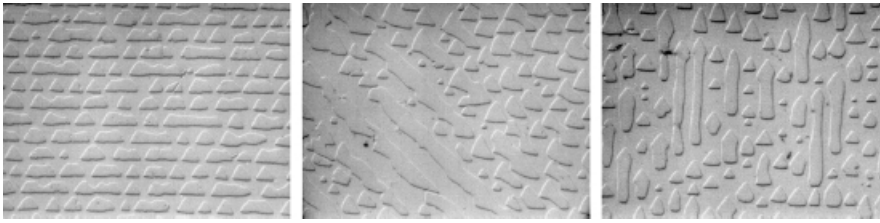


**Fig. 1.** Splitting of ferroelectric domains into triangles at the  $c-$  surface of PPLT for different grating vector orientations; *left:  $k \parallel y$ , center:  $k$  rotated by  $45^\circ$ , right:  $k \parallel x$*

into triangles on the  $c-$  face. The best quality is obtained with  $k \parallel y$ , and therefore this orientation has been used for fabricating crystals used in devices.

The measured nucleation density is  $500 \text{ mm}^{-2}$  in plain congruent lithium tantalate, compared to  $1000 \text{ mm}^{-2}$  in congruent lithium niobate. More interesting for QPM applications is the domain nucleation density on a linear metal electrode, which is part of a periodic pattern. In this case, the nucleation density is  $0.2 \mu\text{m}^{-1}$  for a  $1\text{-}\mu\text{m}$ -wide metal electrode repeated every  $4.75 \mu\text{m}$ . This value is smaller by a factor of 5 compared to PPLN [11], and it varies only slightly with the metal and the method of deposition used for electrode fabrication.

The measurement of the domain wall propagation velocity can provide important knowledge with regard to finding the best poling condition for fabricating short periods [11]. We have found, however, that the sample-to-sample variation of the measured coercive field is larger than the interval of field strength in which the largest change of the velocity occurs. Therefore, it is not possible to obtain a reproducible duty cycle of poled and unpoled material when a constant voltage power supply is used. This difficulty is overcome by using a constant current source rather than a voltage source for poling. In this case the field across the crystal is automatically adjusted to a value near the coercive field.

## 2 Fabrication of PPLT

### 2.1 Lithographic preparation of the electrode structure

In contrast to PPLN, which can be fabricated with either metal or liquid electrodes, metal lines are mandatory for PPLT because of the low domain nucleation density. The preparation of an electrode structure as shown in Fig. 2 is critical to the quality of the poled crystal.

Lithium tantalate wafers are cleaned by plasma etching in oxygen at 10 Pa and in a 400 V bias field to ensure adhesion of either photoresist or chromium in the following processing steps: The wafer is coated with Shipley 1805 photoresist, and the electrode pattern is exposed into the resist. A 100-nm-thick chromium layer is sputtered onto the crystal. The resist is removed with acetone, leaving only the desired electrode structure on the surface of the crystal. The chromium layer thickness is not critical. Much thinner lines have too little conductivity, while thicker lines are more difficult to fabricate using the lift-off technique. The smallest obtained linewidth is  $0.4 \mu\text{m}$ . Since the wavelength of our lithography light source is  $0.31 \mu\text{m}$ , this can be regarded as the technical limit due to diffraction. The electrode structure is covered with a  $6\text{-}\mu\text{m}$ -thick layer of Hoechst 4562 photoresist. Every 8 mm in the  $x$ -direction, a contact window is exposed into

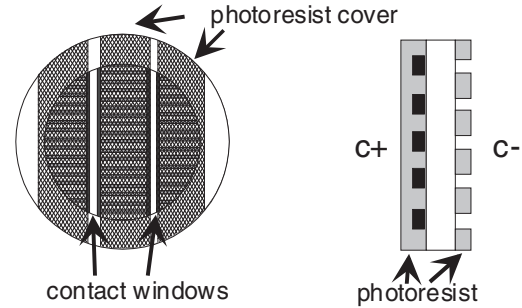


**Fig. 2.** Arrangement of metallic electrodes on the lithium tantalate wafer. In the view from the top (*left*) the metal exposed to the electrolyte is shown in *black* and the metal grating covered by insulating photoresist is *dark grey*. On the  $c-$  face, the photoresist openings correspond to the metal lines on the  $c+$  face, as indicated in the view from the side (*right*)

the resist. Larger spacing than this can lead to interruptions in the periodic domain structure due to excessive resistance within the chromium line, which is estimated to be  $13 \text{ k}\Omega$  for a  $1\text{-}\mu\text{m}$ -wide and  $4\text{-mm}$ -long line. The resist is hard baked in a ventilated oven at  $150^\circ\text{C}$ . This temperature was determined experimentally. Lower temperature yields a resist layer with a conductivity that is too high and has unsatisfactory chemical strength. At higher temperatures, the resist does not have sufficient dielectric strength. After finishing the electrode structure on the  $c+$  face, the  $c-$  face is cleaned and coated with Shipley 1805 resist. The same mask is used to define the electrode structure on the  $c-$  face. This requires a mirror symmetry in the mask layout, but this is not a limiting condition for mask fabrication. During exposure, the mask is aligned parallel to the grating on the  $c+$  face. Both the contact bars and the observation of the moiré effect can be used to confirm parallelism. The phase shift of the mask relative to the electrode pattern on the  $c+$  face cannot be controlled; however, it turned out not to be critical. A sketch of the electrode design is shown in Fig. 2.

### 2.2 E-field poling

For  $E$ -field poling, the patterned lithium tantalate wafer is held in a plexiglass fixture using silicone rubber o-rings. Both crystal surfaces are contacted with a solution of lithium chloride in water ( $120 \text{ g/l}$ ). A function generator and a TREK 20/20 high-voltage amplifier are used as a current source. Initially, a field of  $23 \text{ kV/mm}$  is incident on the crystal, but as soon as a small fraction of the crystal ( $< 10\%$ ) is poled, the current reaches the current limit of the amplifier at  $23 \text{ mA}$ , and the field drops to  $20.8 \text{ kV/mm}$ . The calculated amount of charge required for 50% duty cycle domain inversion determines the actual length of the current pulse. We used a spontaneous polarisation of  $P_s = 0.52 \text{ cm}^{-2}$  to calculate the

necessary charge. For a full wafer with a poled region of 40 mm diameter, the duration of the current pulse is 23 ms. The targeted amount of charge is obtained with better than 1% accuracy. At the end of the poling pulse, the field is switched down to 18 kV/mm, then ramped down to zero within 0.02 s. If the field is switched off immediately and the crystal surfaces come into electrical contact, the domains reverse to their original orientation except small domains at the surface of the crystal. This back switching is also observed in LiNbO<sub>3</sub>. An electrical diode consisting of a series of twenty N4007 diodes completely avoids back switching of domains.

The width of the electrodes has been optimized empirically. Electrodes that are too wide cause domains which are wider than the 50% duty cycle and unpoled areas due to insufficient nucleation density. Electrodes that are too small cause excessive splitting of domains into triangles. A wafer with sections of electrode gratings with different widths between 0.8  $\mu\text{m}$  and 1.8  $\mu\text{m}$ , but a constant poling period of 4.8  $\mu\text{m}$ , was poled in one step, i.e. all experimental parameters are held constant except the electrode width. The uniformity of domain walls is better for wider electrode lines, but it is not possible to obtain a duty cycle of 50%. We found that with the charge necessary for poling a 50% duty cycle using wide electrodes, only a part of the crystal was periodically poled with a larger duty cycle, while a lot of spots were not poled at all. In Fig. 3, two extreme examples are shown for 0.8- $\mu\text{m}$ -wide (left image) and 1.8- $\mu\text{m}$ -wide (right image) electrodes.

Some applications, such as widely tunable optical parametric oscillators (OPOs) [13], require QPM crystals with individual channels of different poling periods. In order to obtain a uniform domain duty cycle of 50% over the entire device, the width of the electrodes has to be adjusted to the poling period. The result of this experimental adjustment is

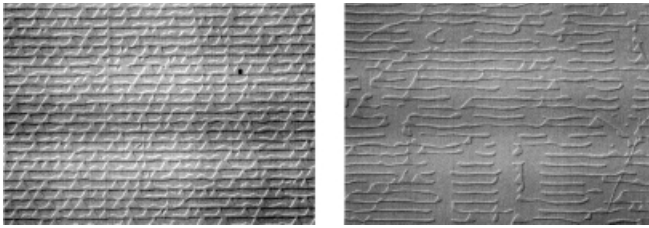


**Fig. 3.** Domain shape on  $c$ -face for 0.8- $\mu\text{m}$ -wide (left) and 1.8- $\mu\text{m}$ -wide (right) electrodes. The period is 4.75  $\mu\text{m}$

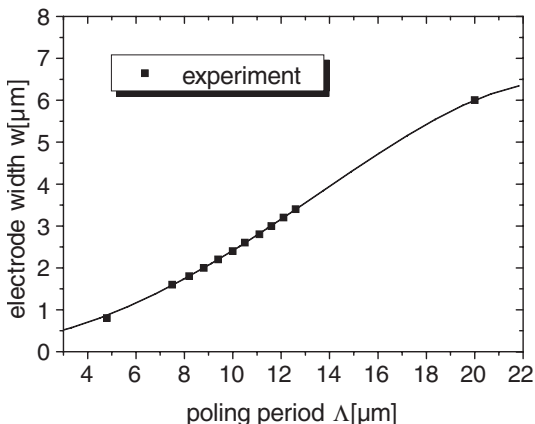


**Fig. 4.** Empirical law for optimum electrode width

**Table 1.** Some values for electrode linewidth,  $w$

QPM period, $\Delta$ ( $\mu\text{m}$ )	1.3	2	3	4	5	8	12	18
Linewidth, $w$ ( $\mu\text{m}$ )	0.3	0.4	0.5	0.7	0.9	1.8	3.2	5.5

shown in Fig. 4. Some values are also given in Table 1. Note that these are the linewidths for the mask. For the very narrow lines below 1  $\mu\text{m}$ , the actual electrodes are slightly wider due to the fabrication process. Using these data, we have fabricated a PPLT crystal with 62 individual QPM channels with periods ranging from 7.5  $\mu\text{m}$  to 13.4  $\mu\text{m}$ . The duty cycle in each channel is constant within 5%. Such a crystal is used for a widely tunable OPO pumped at 532 nm [13]. The goal is to cover the entire IR transparency range from 600 nm to 5  $\mu\text{m}$  with either the signal or the idler output using a single device.

### 3 Optical characterization

#### 3.1 Nonlinear coefficient

A 0.2-mm-thick, 16-mm-long PPLT crystal with a 1.5  $\mu\text{m}$  poling period was fabricated for SHG at 670 nm. The nonlinear optical performance of this crystal was characterized with a single-mode dye laser. The effective nonlinear coefficient was determined by comparing the measured output power with the theoretically expected output power for single-pass SHG under confocal focusing [14]. The effective nonlinear coefficient is  $d_{\text{eff}} = 4.7$  pm/V, which is half of the theoretical

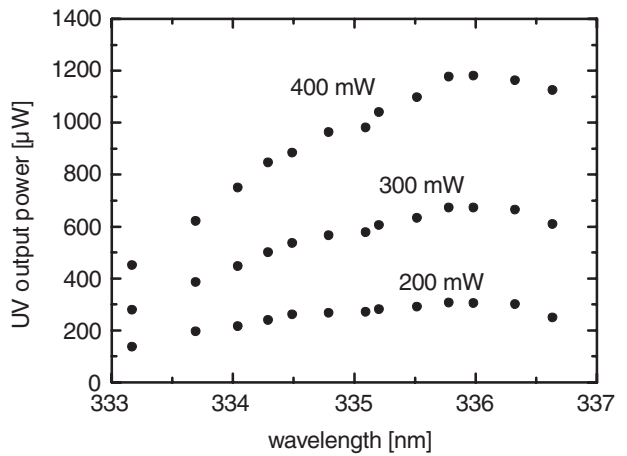


**Fig. 5.** Output power versus wavelength tuning

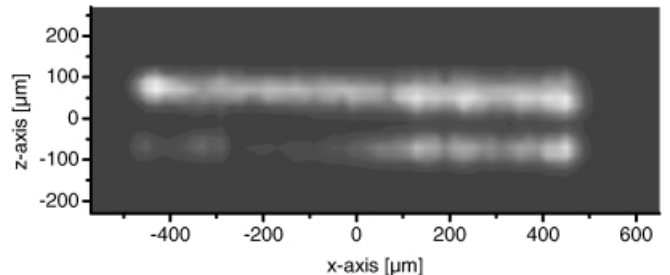


**Fig. 6.**  $x$ - $z$  scan of nonlinear conversion efficiency

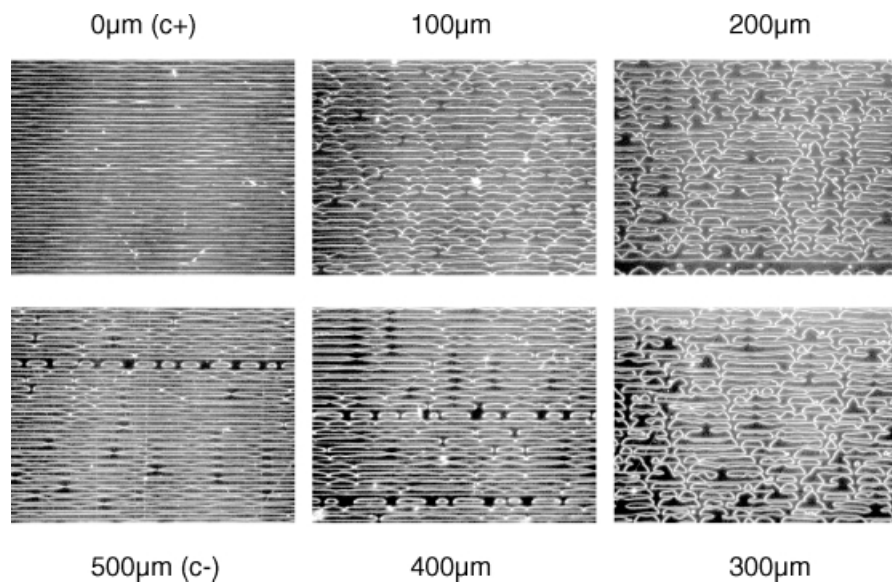


**Fig. 7.** Structure of domains in a 500- $\mu\text{m}$ -thick PPLT crystal at different depths. For further details, see text

value. Nonuniform domains and absorption of UV light both cause the decreased value for  $d_{\text{eff}}$ .

### 3.2 SHG of the diode laser

The diode laser system used for UV generation in PPLT consisted of an SDL 7311-G1 single-mode laser and an SDL 7360-E tapered amplifier. The total output power at 670 nm is 500 mW in a nearly diffraction limited beam. The line width is below 10 MHz, and the wavelength is tunable over a 10 nm range.

The UV output power from the PPLT crystal grows quadratically with the input power as expected from theory. The UV wavelength is tunable from 333.0 nm to 336.8 nm by changing the diode laser wavelength and adjusting the PPLT crystal temperature for phase-matching, while using a fixed position in the crystal. The UV output power as a function of crystal temperature and input power is plotted in Fig. 5. At crystal temperatures below 180 °C, photorefractive effects are observed and the conversion efficiency is decreased. A wider wavelength tuning would be possible by using multi-grating crystals and an oven which can be heated above 200 °C.

### 3.3 Lateral homogeneity

The conversion efficiency as a function of lateral beam position was monitored in the  $x$ - $z$  plane with a spatial resolution of 20  $\mu\text{m}$ . The result is shown in Fig. 6.

The highest conversion efficiency is observed near the  $c+$  surface, i.e. where the domains have been nucleated by the electrodes. A second stripe of good conversion is observed near the  $c-$  face of the crystal. In the bulk of the crystal, the conversion efficiency is significantly decreased. Similar effects are observed in all crystals poled by the double-sided electrode method, but they are less pronounced for longer periods. A 0.5-mm-thick crystal with 4.75  $\mu\text{m}$  poling period was polished at an angle, and the domains have been photographed at different depth in the bulk, as shown in Fig. 7. In the center the domains are less uniform than near the electrodes and therefore the effective nonlinearity is smaller.

## 4 Conclusion

The fabrication of PPLT with short QPM periods has been described. By using electrodes on both crystal surfaces during  $E$ -field poling, the quality of the poled crystals is improved and the fabrication of shorter periods down to 1.3  $\mu\text{m}$  is possible. Further reduction of poling periods will require electrode widths smaller than 0.4  $\mu\text{m}$ , which are difficult to fabricate with conventional optical lithography. The laminar domains of PPLT tend to split into triangles at an aspect ratio of domain height to domain width larger than 100. By using double-side electrodes for  $E$ -field poling, a usable aspect ratio of approximately 200 can be obtained. Larger aspect ratios are possible to fabricate; however, these crystals have a region of decreased conversion in the bulk, while the conversion is best near the surfaces.

*Acknowledgements.* We thank the Bundesministerium für Forschung und Technologie, and the Air Force Office of Scientific Research, for financial support.

## References

1. J.A. Armstrong, N. Bloembergen, J. Ducuing, P. Pershan: *Phys. Rev.* **127**(6), 1918 (1962)
2. M.M. Fejer, G.A. Magel, D.H. Jundt, R.L. Byer: *IEEE J. Quantum Electron.* **QE-28**, 2631 (1992)
3. M. Yamada, N. Nada, M. Saitoh, K. Watanabe: *Appl. Phys. Lett.* **62**, 435–436 (1993)
4. L.E. Myers, R.C. Eckhard, M.M. Fejer, R.L. Byer: *J. Opt. Soc. Am. B* **12**, 2102 (1995)
5. R.G. Batchko, M.M. Fejer, R.L. Byer, D. Woll, R. Wallenstein, V.Y. Shur, L. Erman: *Opt. Lett.* **24**, 1293–1295 (1999)
6. S. Wang, V. Pasiskevicius, L.F. Laurell, H. Karlsson: *Opt. Lett.* **23**, 1883–1885 (1998)
7. F.C. Zumsteg, J.D. Bierlein, T.E. Gier: *J. Appl. Phys.* **47**(11), 4980–4985 (1976)
8. K. Mizuuchi, K. Yamamoto: *Opt. Lett.* **21**, 107 (1996)
9. J.-P. Meyn, M.M. Fejer: *Opt. Lett.* **22**(16), 1214 (1997)
10. P.A. Champert, S.V. Popov, J.R. Taylor, J.-P. Meyn: *Opt. Lett.* **25**, 1252–1254 (2000)
11. G.D. Miller: PhD thesis, Stanford University (1996)
12. V. Gopalan, T.E. Mitchell: *J. Appl. Phys.* **85**(4), 2304–2311 (1999)
13. U. Strössner, A. Peters, J. Mlynek, S. Schiller, J.-P. Meyn, R. Wallenstein: *Opt. Lett.* **24**(22), 1602–1604 (1999)
14. V. Pruneri, S.D. Butterworth, D.C. Hanna: *Opt. Lett.* **21**(1), 390 (1996)